

# Structural Behavior of Concrete One-Way Slab with Mixed Reinforcement of Steel and Glass Fiber Polymer Bars under Fire Exposure

**Mohammed R. Rasheed**

Department of Civil Engineering, Engineering College, University of Baghdad, Iraq  
mohammed.zaed2101m@coeng.uobaghdad.edu.iq (corresponding author)

**Shatha D. Mohammed**

Department of Civil Engineering, Engineering College, University of Baghdad, Iraq  
shatha.dh@coeng.uobaghdad.edu.iq

Received: 21 December 2023 | Revised: 3 February 2024 | Accepted: 11 February 2024

Licensed under a CC-BY 4.0 license | Copyright (c) by the authors | DOI: <https://doi.org/10.48084/etasr.6795>

## ABSTRACT

Steel Reinforced Concrete (RC) frequently faces durability problems. In certain areas, Glass Fiber-Reinforced Polymer (GFRP) rebars are considered a non-corrodible substitute for steel reinforcement. Elevated temperatures have a significant impact on the mechanical characteristics and the adhesiveness of GFRP rebars to concrete, particularly when the polymeric matrix's glass transition temperature is approached or surpassed. Three simply supported reinforced concrete slabs were considered in the experimental program. Each specimen had identical dimensions of 1500×540×120 mm. For the fire resistance requirements, a 45 mm clear concrete cover and an exception of a 200 mm unexposed (cool) anchor zone at the ends were considered. The GFRP replacement ratio was 0, 20, and 40%. The burning procedure involved fire exposure for an hour with a steady-state temperature of 500 °C in accordance with ASTM E-119 regarding the temperature time elevation and a sudden cooling condition. The optimal concrete cover was detected by testing a fire-exposed small model reinforced by GFRP bars of varying concrete cover. The specimen was tested under static intense loads. The reference slab and the slab with a replacement percentage of 20% failed due to flexural failure, whereas the slab with a replacement percentage of 40% failed due to shear failure. The influence of the GFRP replacement ratio was extended to include toughness and ultimate load. A replacement percent of 20% increased them by 18.30, and 2.62%, respectively, while a replacement percent of 40% decreased them by 28.16, and 3.13%, accordingly. It was also shown that the location of replacing the GFRP and 200 mm of unexposed (cold) installation area at the ends with a 45 mm concrete cover has a significant impact. The more the GFRP is located in the middle, away from the ends, the better the fire resistance is.

*Keywords-reinforced concrete slabs; fire resistance; Glass Fiber-Reinforced Polymer (GFRP); concrete cover*

## I. INTRODUCTION

Over the past ten years, Fiber-Reinforced Polymer (FRP) materials have attracted increasing attention in civil engineering research. The original applications for FRPs were in the chemical processing, automotive, and aerospace industries. High strength-to-weight ratios and corrosion resistance are just two of their advantages, which make them desirable for usage in a wide range of civil engineering applications. There are many FRP field applications due to advancements in knowledge and FRP technology, and the rise in their utilization. These developments have also decreased material cost and increased structural designers' trust. FRPs show significant potential across various applications, with a notable impact on internal concrete reinforcement. In this role, FRPs can effectively substitute traditional steel reinforcement, providing a solution to combat electrochemical corrosion.

Electrochemical corrosion has substantially contributed to the ongoing global infrastructure crisis and the deterioration observed in reinforced concrete structures over the last 50 years [1-6]. The performance of FRP-reinforced concrete structures has been the subject of numerous studies [7-15]. However, research indicates that FRP-reinforced concrete slabs usually fracture abruptly and unevenly. The combination of FRP with steel bars, specifically by placing Glass Fiber-Reinforced Polymer (GFRP) at the ends of a structure, emerges as an effective method to prevent corrosion of stainless steel within the construction. This integration acts as a preventive measure, strategically inhibiting the corrosion of stainless-steel components in the structure. The benefits of both FRP and steel bars enhance the overall performance of the slab. Many researchers have explored the performance of concrete structures reinforced with this combination [16-18].

As its name implies, FRPs are composed of tiny fibers embedded in a polymer matrix. Epoxies, polyesters, or vinyl esters, which are typically carbon (graphite), glass, or aramid (Kevlar), are commonly employed as matrices for the fibers used in civil engineering. The mechanical and thermal properties of FRPs are greatly influenced by temperature, and even a slight rise in temperature (between 100 and 200 °C) can result in a discernible deterioration in the FRPs' mechanical qualities [1]. FRP-reinforced parts' fire endurance can be affected by a number of factors, including the type of reinforcement used, the type of aggregate utilized, and the thickness of the concrete cover. With different FRP materials exhibiting varying degrees of mechanical and bond property degradation at high temperatures, the kind of reinforcement is a crucial factor to take into account [19]. The type of aggregate and the concrete cover have a significant impact on the heat transfer to the reinforcement, which in turn influences the temperatures in the exposed and anchoring zones of the bars during a fire [19].

Before the most recent edition of ACI 440.1R (ACI 2015), the use of FRP reinforcing bars was not advised in circumstances where maintaining structural integrity in the face of fire was critical [19]. Experimental research, however, has raised expectations for GFRP bars' fire performance [20-21]. CSA S806 [22] recommends being cautious and using a thick concrete cover (e.g. 45 mm for 1 hr of fire resistance) to prevent GFRP bars from deteriorating during a fire.

Authors in [22] delved into assessing the fire resistance of concrete slabs reinforced with FRP. Their research encompassed numerical parametric analysis and a comprehensive review of the existing literature in this domain. The investigation specifically employed numerical finite difference analysis to scrutinize the time-temperature response of a concrete slab internally reinforced with FRP under fire exposure. Upon thorough examination of the limited available literature, the authors concluded that, when reaching a critical temperature of 250°C in the internal FRP reinforcement, certain effects or behaviors were observed. The numerical approach graded fire endurance and represented the worst-case scenario for GFRP. The study discovered that thicker concrete covers, carbonate aggregate concrete, and FRP-reinforced concrete slabs have higher fire endurance than slabs reinforced with conventional reinforcing steel. It was also found that material property data for FRPs at elevated temperatures are required, and structural fire endurance tests are necessary to validate the numerical models. In [24], the impact of various reinforcement techniques on the firing behavior of RC beams under service load was analytically investigated. When a beam's resistance could no longer sustain the service load, the beam failed. A steel beam shattered after 100 min of fire, but a Carbon Fiber-Reinforced Polymer (CFRP) beam withstood the heat for 60 min. However, after being exposed to fire for 40 minutes, the GFRP-RC and AFRP beams crumbled.

Authors in [21, 25] conducted an experimental research, which showed that fire-exposed GFRP-RC slab bond failure can be avoided by providing sufficient anchorage of bars with extended unexposed (cool) portions. Although previous experimental research raised concerns regarding fire safety and

GFRP bar application in concrete, these findings may reduce bond failure in fire-exposed GFRP-RC slabs. Two GFRP RC slabs containing carbonate and siliceous coarse aggregates were tested in [26]. With temperatures 10% lower than the slab with siliceous aggregates, the slab with carbonate aggregates fared better in the fire. The authors conducted numerical parametric investigations on slabs, including those two aggregates as well as expanded shale aggregates as a result of their findings. The enlarged shale aggregate slabs demonstrated a fire resistance of 85 min with a 50 mm suggested cover, followed by siliceous (65 min) and carbonate (72 min) slabs. GFRP-RC slabs with cover thicknesses of 25 and 38 mm were tested in a fire scenario without any load in [27]. As predicted, after 4 hr of fire exposure, the bottom temperatures of the longitudinal rebars varied significantly, with a lower slab having 100 °C higher temperature than the higher slab.

The literature study presented above emphasizes a few crucial findings: (i) the thickness of the concrete cover significantly impacts GFRP-RC elements' thermal response, (ii) concrete elements containing carbonate aggregates fare slightly better in fires than those made with siliceous aggregates, (iii) overall slab thickness does not appear to significantly affect fire behavior, (iv) while comparative studies are limited, CFRP-RC elements generally perform better than GFRP-RC elements, though the results are not very clear, (v) the bond between FRP reinforcement and concrete greatly affects fire behavior, bent rebars at the far end of the anchorage can increase fire resistance, and (vi) lap splices in FRP rebars significantly affect the fire resistance of FRP-RC beams.

According to the outcomes of the literature review concerning the structural behavior of GFRP-reinforced concrete elements under fire exposure, it was concluded that the support location would be damaged, and the fire effect would cause local failure. The current analysis aims to offer valuable insights into the slab post-fire behavior, especially with mixed reinforcement while considering different GFRP replacement ratios of 0, 20, and 40%, defining an optimized combination of a 45 mm thick concrete cover and a 200 mm unexposed (cold) fixation area at the end to improve the structural behavior. Examining the test results includes assessing critical aspects, such as ultimate load capacity, load-deflection behavior, load-strain relationships, and the material's toughness.

## II. EXPERIMENTAL PROGRAM

### A. Materials

The casting of all samples and control specimens involved the utilization of Ordinary Portland Cement (CEM I 42.5R) obtained from the Mass brand in Iraq. An evaluation of the cement's adherence to the Iraqi Specification No. 5/2019 [28] was conducted. The chosen sand was classified as belonging to Zone 2. The siliceous aggregates utilized in the study consisted of crushed gravel with a maximum particle size of 12 mm. Both fine and coarse aggregates exhibited conformity with the Iraqi Specification (IQS) No. 45/1993 [29]. The details about the combinations can be found in Table I. The specifics of the utilized GFRP and steel bars are presented in Table II.

TABLE I. DETAILS OF CONCRETE MIX PROPORTIONS.

Cement (kg/m <sup>3</sup> )	Gravel (kg/m <sup>3</sup> )	Sand (kg/m <sup>3</sup> )	Water (l/m <sup>3</sup> )	Optima 100 (kg/m <sup>3</sup> )	Silica fume (kg/m <sup>3</sup> )	Specimen strength f <sub>cu</sub> (MPa)
470	945	827	170	6.2	20	54

TABLE II. THE PROPERTIES OF REINFORCEMENT BARS.

Bars	Nominal diameter (mm)	Tensile strength (MPa)	Modulus of elasticity E, (MPa)	Elongation (%)
GFRP	10	1207	48280	2.5
Steel	10	437	200000	11
Steel	8	434	200000	12

B. Concrete Cover Checking

Before the specimens were prepared, a 400 × 210 × 110 mm miniature model with a compressive strength of f<sub>cu</sub> = 40 MPa was cast and reinforced by four GFRP bars, the mix proportion is displayed in Table III. As discerned in Figure 1, the model was cast on a variety of concrete covers. The model was coated with water-soaked canvases that were sprayed every day. The miniature model was then subjected, in compliance with ASTM E-119, to fire at a steady-state temperature of 500 °C for 1 hr (Figure 2). When the fire exposure ended, rapid cooling technique (water spraying) was used to chill the model. After that, as observed in Figure 3, the model was broken and the GFRP bars were removed. The GFRP bars on the sides were seen to be burned, and it was discovered that the middle cover, which was 45 mm from the bottom, best prevented burning.

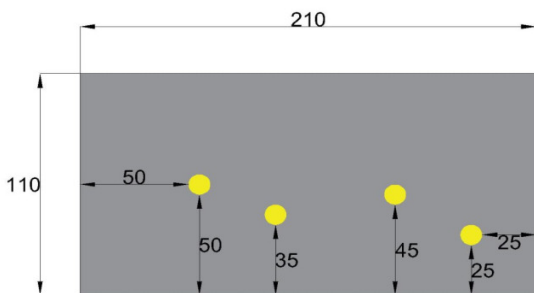


Fig. 1. Dimensions of a miniature model (mm).

TABLE III. MIXTURE SPECIFICATIONS FOR THE ADOPTED COMPRESSIVE STRENGTH MODEL

Water (kg/m <sup>3</sup> )	Cement (kg/m <sup>3</sup> )	Sand (kg/m <sup>3</sup> )	Gravel (kg/m <sup>3</sup> )	f <sub>cu</sub> (MPa)
200	400	755	1002	40



Fig. 2. Casting and burning of the miniature model.

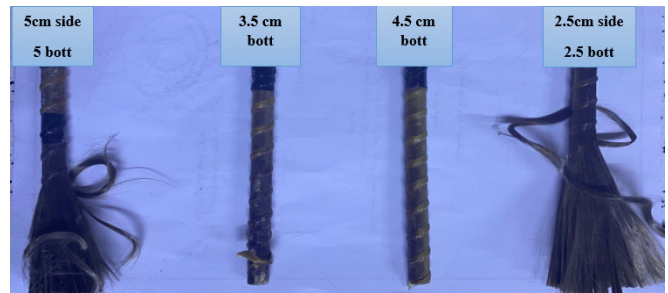


Fig. 3. Condition of the GFRP bars after exposure to fire.

C. Tested Specimens

The experimental program included testing three identical concrete slabs with the same geometric layout and concrete compressive strength. Each slab was 1500 mm, 550 mm, and 120 mm in length, width, and depth, respectively. Additional details regarding the test specimens are portrayed in Figure 4 and Table IV.

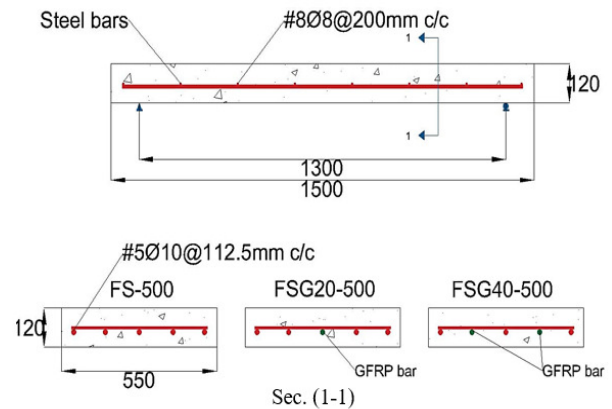


Fig. 4. Dimensions and reinforcement details of the specimens.

TABLE IV. CHARACTERISTICS OF THE TESTED SPECIMENS.

Slab designation	f <sub>c</sub> ' MPa	Temperature (°C)	GFRP ratio (%)
FS-500	43	500	0
FSG20-500	43	500	20
FSG40-500	43	500	40

D. Burning and Cooling

As shown in Figures 5 and 6, the specimens were set inside a gas furnace and were exposed to a direct flame for 1 hr while keeping the temperature steady at 500±10 °C. A digital thermometer reader fitted with sensor wire type K was used to track the temperature of the specimen and furnace region, according to ASTM E-119 [30]. The specimens were sprayed with water (sudden cooling) to lower their temperature after the burning procedure.

D. Testing Procedure

Two hemispherical supports, intended to offer straightforward support, were attached to the slabs. The length of the slabs under examination and the measurement of the distance between the supports were 1300 mm. After that, a 100-ton hydraulic jack was used to apply the load. A steel

loading, I-section girder equally distributed the load, producing two equal forces divided by a 400 mm span. Several measurements were made during the experiment, including the strain experienced by the concrete surface, the applied load amplitude, and the vertical deflection at the center of the slab. Every stage of the loading procedure involved recording of these measurements. Each phase of the load process entailed a 2.5 kN increase until failure occurred. The crack formation was meticulously monitored and recorded following each step. See Figures 7-9 for a more thorough explanation of the experimental setup.



Fig. 5. Setup of the furnace and specimens.

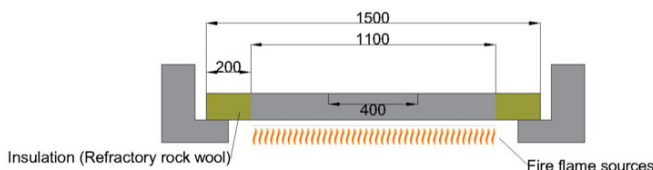


Fig. 6. Fire test setup (mm).

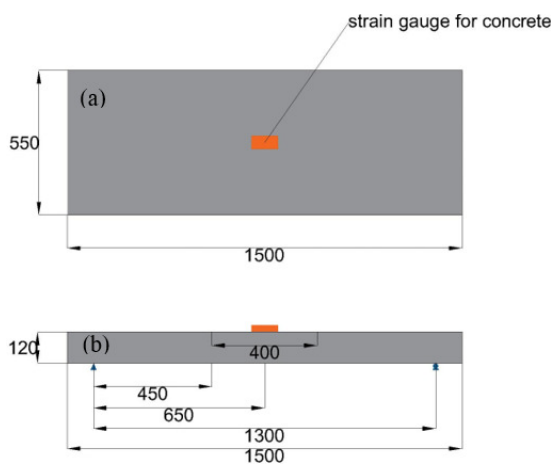


Fig. 7. Locations of the strain gauge: (a) Top face, (b) side face (mm).

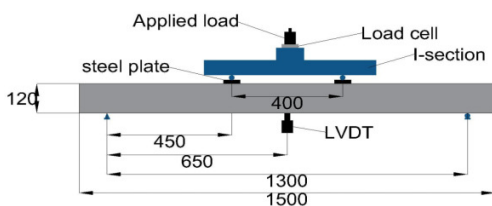


Fig. 8. Details of the test setup (mm).

### III. TEST RESULTS AND DISCUSSION

An application of a two-point load was utilized to test three reinforced concrete slabs with different ratios of GFRP bars in place of steel bars as depicted in Figure 9. The load was increased steadily until the point of failure. The discussion comprised four categories to enhance the comprehension of the slab's structural behavior. These are:

- Crack pattern, failure load, and mode of failure.
- Load–deflection behavior.
- Load-strain relation.
- Toughness.

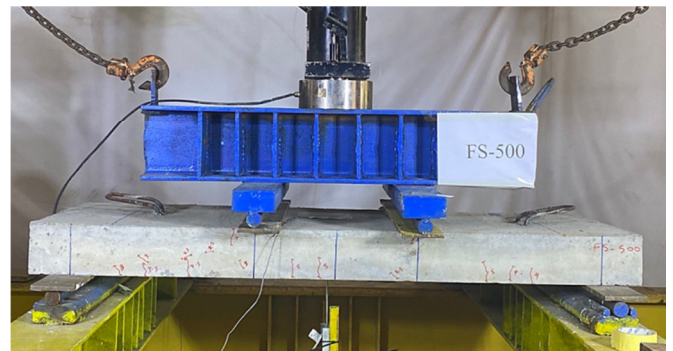


Fig. 9. Test setup.

#### A. Cracks Pattern, Failure Load, and Mode of Failure

The results for the burned specimens revealed that, after the firing and cooling process, cracks began to occur on the slabs' surfaces. Flexural cracks were also developed as an outcome of the fire in the slabs' sides and bottom. Once the burning and cooling procedure were completed, the specimens were put through a two-line static load test. As exposed in Table V, the variation in the ultimate load for the specimen FSG20-500 was +2.62% compared to the reference slab, whereas it was decreased by 3.13% for the specimen FSG40-500. The reduction in strength and mechanical properties of concrete material prevents the flexural reinforcement from reaching its maximum ultimate strength. Consequently, no significant influence was observed regarding the effect of glass fiber bars.

The slabs FS-500 and FSG20-500 experienced flexural failure while the slab (FSG40-500) experienced shear failure. First, additional cracks that emerged from fire fractures in the slab's bottom face were created. Flexural cracks spread along the bottom surface of the reference slab FS-500 and the slab with a replacement percent of 20% (FSG20-500), in a direction parallel to the support direction and the original crack as the stress increased. Cracks began to appear at the failure stage, ultimately spreading to the sides of the slab and the compression chord. The cracks were located in the central third of the slab. None was observed in the vicinity of the supports. The final specimens' breaking pattern is spotted in Figures 10 and 11. These figures unequivocally demonstrate that no fractures were observed in the area of support zones and that flexural cracks are roughly parallel to one another.

TABLE V. LOAD CAPACITY AND ULTIMATE DEFLECTION OF THE BURNED SPECIMENS

Specimen	Ultimate deflection (mm)	Ultimate load (kN)	% Variation of ultimate load (with respect to FS-500)
FS-500	49.445	69.3	---
FSG20-500	56.5708	71.12	+2.62
FSG40-500	41.3141	67.13	-3.13

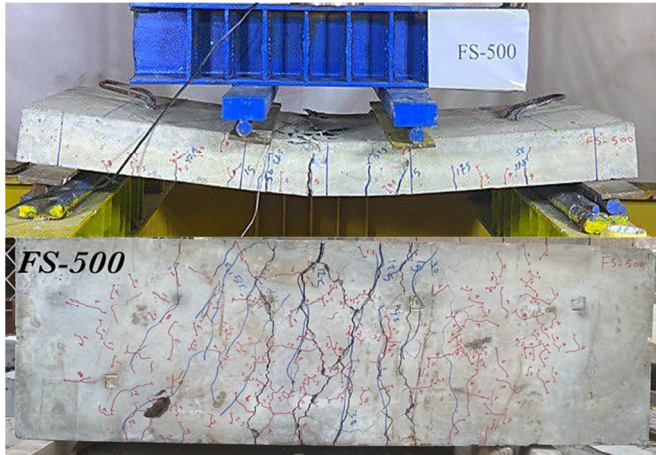


Fig. 10. Crack pattern of the specimen FS-500. Top: side face, bottom: bottom face.



Fig. 11. Crack pattern of the specimen FSG20-500. Top: side face, bottom: bottom face.

In the slab FSG40-500, in which the substituted ratio was 40%, the pattern of the cracks was completely different. As the applied load increased, more flexural fracture development and propagation were observed on the slab's bottom surface. The supports' orientation and the initial fracture were parallel to one other. Subsequently, diagonal shear cracks started to propagate along the slab's sides. When the applied load was gradually increased, the shear fractures in the slab seemed to get larger and travel toward the loading location. As soon as the diagonal shear cracks were generated by the debonding of the GFRP bars, the slab collapsed. Due to the 40% replacement percent (2 from 5 bars) that increased the slab's flexural resistance, shear failure mode rather than flexure mode occurred.



Fig. 12. Crack pattern of the specimen FSG40-500. Top: side face, bottom: bottom face.

B. Load-Deflection Behavior

Every load increment during the test procedure involved measuring the deflection at the slab center. The service and ultimate load phases were examined for sample deflection. It is generally assumed that the service load accounts for around 70–75% of the total load [31]. In the current experiment, the service load for each specimen was determined to be the 70% of the ultimate load. The specimens' ultimate loads were calculated based on the maximum bearing load, as illustrated in Table V. Throughout the incremental loading process, several distinct phases were generally observed. In the elastic zone, the deflection first increased gradually and steadily. When cracks began to develop and spread, the deflection rate quickened and accelerated. The deflection curve's slope then started to decline as this pattern persisted until the tension stress in the steel reinforcement reached its yield point. The test is declared to be terminated when the deflection keeps rising without the applied load increasing in proportion. Figure 13 exhibits how the GFRP bar percentage adjustments affect the mid-span load-deflection characteristics. FS-500 serves as the control sample, and the outcomes of the specimens FSG20-500 and FSG40-500 are compared with it. The load-deflection curves evidents that the three slabs' degrees of stiffness vary inside the elastic zone. Table VI showcases the specimens' rigidity (stiffness) at the elastic zone. The results indicate that the stiffness decreased by about 5.18 and 21.29% for a replacement percent of 20 and 40%, respectively.

TABLE VI. STIFFNESS OF THE TESTED SPECIMENS

Specimen	Load (kN)	Deflection at 20 kN load	Stiffness $K=P/\Delta$ (kN/mm)	Stiffness decrease (%)
FS-500	20	3.7	5.40	---
FSG20-500	20	3.9	5.12	5.18
FSG40-500	20	4.7	4.25	21.29

TABLE VII. MID-SPAN DEFLECTIONS OF THE TESTED SAMPLES AT SERVICE AND ULTIMATE LOADS

Specimen	Deflection at service load (mm)	% Increase in deflection at service load	Deflection at ultimate load (mm)	% Change in deflection at ultimate load
FS-500	9.3	Ref.	49.44	Ref.
FSG20-500	11.3	21.50	56.57	+14.4
FSG40-500	14.2	52.68	41.31	-16.45

The discrepancy is attributed to the different moduli of elasticity of the steel and GFRP, with the GFRP having a lower modulus of elasticity than the steel, given that all the other parameters of the specimens studied are compatible. In comparison to the control slab, this causes the load-deflection curve for the GFRP-reinforced slab to have a lower initial slope. These results validate the conclusions obtained in [32].

The trend of the load-deflection comprised two stages. The behavior before the steel reinforcement yield point constitutes the first stage. At this stage, the replacement of 20% demonstrated a behavior slightly similar to that of the reference slab, with an insignificant decrease in stiffness. There was an increase in the deflection, which led to a decrease in stiffness. As for the case of 40% replacement, the deflection increased prominently in the elastic region, and this led to a significant reduction in stiffness and deterioration of the concrete in the elastic region. This difference between the modulus of elasticity of steel and GFRP caused this jump in the structural behavior, as the GFRP has lower modulus of elasticity than steel. In the second stage, which starts after the steel yielding, it can be noticed that the behavior with 20% replacement was similar to that of the reference slab, as the deflection began to increase significantly with a slight increase in the load, i.e. the flexural resistance decreased and led to the flexure failure. In the case of 40% replacement after the point of steel yielding, the GFRP bar had a greater role in increasing load, and the load began to increase with a slight augmentation in deflection. The specimen began to tend toward the brittle (linear) behavior, which is compatible with the GFRP load-strain behavior. This means the flexural resistance increased and led to shear failure.

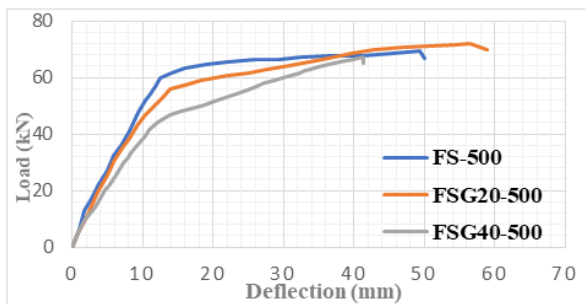


Fig. 13. Load-deflection behavior at mid-span.

C. Load-Strain Relation.

The concrete top surface's strain-load relations were measured at the mid-span. Figure 14 illustrates the effect of increasing the GFRP replacement percentage on the load-strain relations of the top concrete surface at the mid-span. In the elastic zone before the yield of steel reinforcement, the concrete's compressive strain was 710, 802, and 920 micro-strains for specimens FS-500, FSG20-500, and FSG40-500, respectively. This indicates that because steel and GFRP have different elastic moduli, the strain in the elastic area was directly proportional to the replacement ratio. The deflection in the elastic zone increases as the elastic modulus decreases, and the strain in the concrete in the elastic region increases as the deflection increases. The elastic region experienced an increase in strain and a significant decrease in stiffness at 40% material

replacement. Premature shear failure occurred as a result of the concrete's degradation in the elastic zone. The FS-500 specimen had a compressive strain of 4125 micro-strains, the FSG20-500 specimen had a micro-strain of 3362, and the FSG40-500 specimen had a micro-strain of 3220 at the ultimate load.

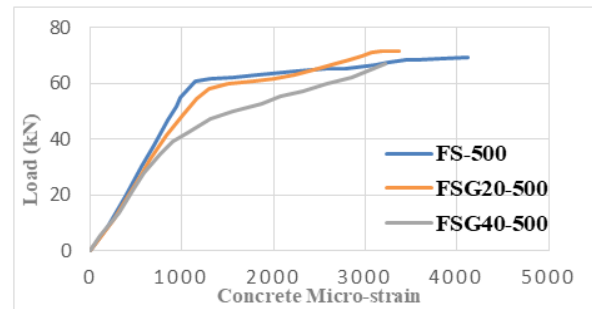


Fig. 14. Load-strain curves for concrete top fiber at the mid-span.

D. Toughness

The integral of the load-deflection curves for the slabs was computed to calculate the flexural toughness, also cited as total energy. Flexural toughness refers to a material's total ability to absorb energy. One important property in the realm of concrete structures is the ability of a loaded structure to store energy. The highest load magnitude and the deflection seen at the point of failure both have an impact on the absorbed energy, which is measured by the area under the load-deflection curve. The total energy of the slabs that were tested is displayed in Table VIII. It is evident that increased load capacity and deflection modified the toughness by 18.30% when 20% of the steel was replaced. Due to the lower deflection and load capacity, the toughness decreased by 28.16% when the replacement ratio was 40%

TABLE VIII. TOUGHNESS OF TESTED SLABS

Specimen	Toughness at ultimate load (kN.mm)	% variation of toughness at ultimate load	Toughness at failure load (kN.mm)	% variation of toughness at failure load
FS-500	2859.72	---	2897.55	---
FSG20-500	3254.28	+13.83	3427.92	+18.30
FSG40-500	1906.84	-27.21	1957.65	-28.16

IV. CONCLUSIONS

In this paper, a set of post-fire experiments was carried out on three reinforced concrete slabs to evaluate their structural performance. The collected data were subsequently analyzed, considering a variety of hybrid reinforcement ratios and placements. The main conclusions of this study are:

- The use of a fire protection process and optimal concrete cover prevent supporting local failure in fire-exposed specimens that contain mixed steel and GFRP reinforcement.
- The location of replaced GFRP bars plays a crucial role. Optimal positioning is essential for enhanced fire resistance. Specifically, placing GFRP more centrally, and

away from the ends, has a positive impact, resulting in superior fire resistance performance.

- To resist a fire of 500 °C for 1 hr, the utilization of 200 mm of unexposed (cold) installation surface at the ends with a 45 mm concrete cover was adequate.
- Increasing the GFRP replacement ratio up to 40% decreased the ultimate load. Consequently, no significant influence was observed regarding the effect of glass fiber, so it is recommended to use high compressive strength when using mixed reinforcement.
- The percentage of 20% replacement of steel reinforcement by GFRP bars did not change the failure mode. It was observed that the majority of the fractures were found in the middle third of the slab. In contrast, no cracks were found near the supports, suggesting flexural failure mode. Moreover, increasing the GFRP replacement ratio up to 40% changed the failure mode to shear failure.
- Since steel has a higher modulus of elasticity than GFRP, the stiffness in the elastic zone for mixed reinforced specimens decreases as the replacement percentage increases.
- A significant effect was absorbed regarding the compressive concrete strain as a mixed reinforcement of steel and GFRP was considered. The effect was directly proportional with the GFRP replacement ratio.
- It is evident that a 20% replacement of GFRP modified the toughness, whereas increasing the replacement ratio to 40% reduced it.

#### REFERENCES

- [1] L. A. Bisby, "Fire behaviour of fibre-reinforced polymer (FRP) reinforced or confined concrete," Ph.D. dissertation, Queen's University, Kingston, CA, USA, 2003.
- [2] T. H. Ibrahim, I. A. S. Alshaarba, A. A. Allawi, N. K. Oukaili, A. El-Zohairy, and A. I. Said, "Theoretical Analysis of Composite RC Beams with Pultruded GFRP Beams subjected to Impact Loading," *Engineering, Technology & Applied Science Research*, vol. 13, no. 6, pp. 12097–12107, Dec. 2023, <https://doi.org/10.48084/etasr.6424>.
- [3] A. Jalil and A. H. Al-Zuhairi, "Behavior of Post-Tensioned Concrete Girders Subject to Partially Strand Damage and Strengthened by NSM-CFRP Composites," *Civil Engineering Journal*, vol. 8, no. 7, pp. 1507–1521, Jul. 2022, <https://doi.org/10.28991/CEJ-2022-08-07-013>.
- [4] M. A. E. Zareef, "An Experimental and Numerical Analysis of the Flexural Performance of Lightweight Concrete Beams reinforced with GFRP Bars," *Engineering, Technology & Applied Science Research*, vol. 13, no. 3, pp. 10776–10780, Jun. 2023, <https://doi.org/10.48084/etasr.5871>.
- [5] B. Abdulkareem and A. F. Izzet, "Serviceability of Post-fire RC Rafters with Openings of Different Sizes and Shapes," *Journal of Engineering*, vol. 28, no. 1, pp. 19–32, Jan. 2022, <https://doi.org/10.31026/j.eng.2022.01.02>.
- [6] H. Q. Abbas and A. H. Al-Zuhairi, "Use of EB-CFRP to Improve Flexural Capacity of Unbonded Post-Tensioned Concrete Members Exposed to Partially Damaged Strands," *Civil Engineering Journal*, vol. 8, no. 6, pp. 1288–1303, Jun. 2022, <https://doi.org/10.28991/CEJ-2022-08-06-014>.
- [7] B. Saikia, P. Kumar, J. Thomas, K. S. N. Rao, and A. Ramaswamy, "Strength and serviceability performance of beams reinforced with GFRP bars in flexure," *Construction and Building Materials*, vol. 21, no. 8, pp. 1709–1719, Aug. 2007, <https://doi.org/10.1016/j.conbuildmat.2006.05.021>.
- [8] Z. Wang, X. Liang, Y. Wang, and T. Zhai, "Experimental and theoretical investigations on the flexural behavior of RC slabs with steel-PVA hybrid fiber reinforced cementitious composite (HFRCC) permanent formwork," *Case Studies in Construction Materials*, vol. 17, Dec. 2022, Art. no. e01432, <https://doi.org/10.1016/j.cscm.2022.e01432>.
- [9] W. Qu, X. Zhang, and H. Huang, "Flexural Behavior of Concrete Beams Reinforced with Hybrid (GFRP and Steel) Bars," *Journal of Composites for Construction*, vol. 13, no. 5, pp. 350–359, Oct. 2009, [https://doi.org/10.1061/\(ASCE\)CC.1943-5614.0000035](https://doi.org/10.1061/(ASCE)CC.1943-5614.0000035).
- [10] C. Barris, L. Torres, J. Comas, and C. Miàs, "Cracking and deflections in GFRP RC beams: An experimental study," *Composites Part B: Engineering*, vol. 55, pp. 580–590, Dec. 2013, <https://doi.org/10.1016/j.compositesb.2013.07.019>.
- [11] A. I. Said and O. M. Abbas, "Serviceability behavior of High Strength Concrete I-beams reinforced with Carbon Fiber Reinforced Polymer bars," *Journal of Engineering*, vol. 19, no. 11, pp. 1515–1530, Nov. 2013, <https://doi.org/10.31026/j.eng.2013.11.10>.
- [12] S. I. Ali and A. A. Allawi, "Effect of Web Stiffeners on The Flexural Behavior of Composite GFRP- Concrete Beam Under Impact Load," *Journal of Engineering*, vol. 27, no. 3, pp. 76–92, Feb. 2021, <https://doi.org/10.31026/j.eng.2021.03.06>.
- [13] A. H. A. Al-Ahmed and M. H. M. Al-Jburi, "Behavior of Reinforced Concrete Deep Beams Strengthened with Carbon Fiber Reinforced Polymer Strips," *Journal of Engineering*, vol. 22, no. 8, pp. 37–53, Aug. 2016, <https://doi.org/10.31026/j.eng.2016.08.03>.
- [14] M. Abas Golham and A. H. A. Al-Ahmed, "Behavior of GFRP reinforced concrete slabs with openings strengthened by CFRP strips," *Results in Engineering*, vol. 18, Jun. 2023, Art. no. 101033, <https://doi.org/10.1016/j.rineng.2023.101033>.
- [15] J. Abd and I. K. Ahmed, "The Effect of Low Velocity Impact Loading on Self-Compacting Concrete Reinforced with Carbon Fiber Reinforced Polymers," *Engineering, Technology & Applied Science Research*, vol. 11, no. 5, pp. 7689–7694, Oct. 2021, <https://doi.org/10.48084/etasr.4419>.
- [16] K. Protchenko, K. Mlodzik, M. Urbanski, E. Szmigiera, and A. Garbacz, "Numerical estimation of concrete beams reinforced with FRP bars," *MATEC Web of Conferences*, vol. 86, 2016, Art. no. 02011, <https://doi.org/10.1051/mateconf/20168602011>.
- [17] H. Y. Leung and R. V. Balendran, "Flexural behaviour of concrete beams internally reinforced with GFRP rods and steel rebars," *Structural Survey*, vol. 21, no. 4, pp. 146–157, Jan. 2003, <https://doi.org/10.1108/02630800310507159>.
- [18] R. A. Hawileh, "Finite element modeling of reinforced concrete beams with a hybrid combination of steel and aramid reinforcement," *Materials & Design (1980-2015)*, vol. 65, pp. 831–839, Jan. 2015, <https://doi.org/10.1016/j.matdes.2014.10.004>.
- [19] *ACI 440.1R-15(2015), Guide for the Design and Construction of Structural Concrete Reinforced with Fiber-Reinforced Polymer (FRP) Bars*. Farmington Hills, MI, USA: ACI Concrete, 2015.
- [20] L. A. Bisby and V. K. R. Kodur, "Evaluating the fire endurance of concrete slabs reinforced with FRP bars: Considerations for a holistic approach," *Composites Part B: Engineering*, vol. 38, no. 5, pp. 547–558, Jul. 2007, <https://doi.org/10.1016/j.compositesb.2006.07.013>.
- [21] E. Nigro, G. Cefarelli, A. Bilotta, G. Manfredi, and E. Cosenza, "Fire resistance of concrete slabs reinforced with FRP bars. Part I: Experimental investigations on the mechanical behavior," *Composites Part B: Engineering*, vol. 42, no. 6, pp. 1739–1750, Sep. 2011, <https://doi.org/10.1016/j.compositesb.2011.02.025>.
- [22] *CSA - S806(2012), Design and construction of building structures with fibre-reinforced polymers*. Toronto, ON, Canada: Canadian Standards Association, 2012.
- [23] V. K. R. Kodur and D. Baingo, "Fire Resistance of FRP Reinforced Concrete Slabs," National Research Council of Canada, Ottawa, ON, Canada, Internal Report No. 758, 1998.

- [24] M. Saafi, "Effect of fire on FRP reinforced concrete members," *Composite Structures*, vol. 58, no. 1, pp. 11–20, Oct. 2002, [https://doi.org/10.1016/S0263-8223\(02\)00045-4](https://doi.org/10.1016/S0263-8223(02)00045-4).
- [25] H. Hajiloo, M. F. Green, M. Noel, N. Benichou, and M. Sultan, "Fire tests on full-scale FRP reinforced concrete slabs," *Composite Structures*, vol. 179, pp. 705–719, Nov. 2017, <https://doi.org/10.1016/j.compstruct.2017.07.060>.
- [26] V. K. R. Kondur and L. Bisby, "Evaluation of fire endurance of concrete slabs reinforced with FRP bars," *Journal of Structural Engineering*, vol. 131, no. 1, pp. 34–43, 2005.
- [27] V. K. R. Kodur, L. A. Bisby, and S. H.-C. Foo, "Thermal Behavior of Fire-Exposed Concrete Slabs Reinforced with Fiber-Reinforced Polymer Bars," *Structural Journal*, vol. 102, no. 6, pp. 799–807, Nov. 2005, <https://doi.org/10.14359/14787>.
- [28] *I.Q.S. No. 5/2019 Specification, Portland Cement*. Baghdad, Iraq: Central Organization for Standardization & Quality Control (COSQC), 2019.
- [29] *I.Q.S. No. 45 Aggregate from Natural Sources for Concrete and Construction*. Baghdad, Iraq: Central Organization for Standardization & Quality Control (COSQC), 1984.
- [30] *ASTM E119-22(2022), Standard Test Methods for Fire Tests of Building Construction and Materials*. West Conshohocken, PA, USA: ASTM International, 2022.
- [31] K. H. Tan and H. Zhao, "Strengthening of Openings in One-Way Reinforced-Concrete Slabs Using Carbon Fiber-Reinforced Polymer Systems," *Journal of Composites for Construction*, vol. 8, no. 5, pp. 393–402, Oct. 2004, [https://doi.org/10.1061/\(ASCE\)1090-0268\(2004\)8:5\(393\)](https://doi.org/10.1061/(ASCE)1090-0268(2004)8:5(393)).
- [32] I. F. Kara, A. F. Ashour, and M. A. Koroglu, "Flexural behavior of hybrid FRP/steel reinforced concrete beams," *Composite Structures*, vol. 129, pp. 111–121, Oct. 2015, <https://doi.org/10.1016/j.compstruct.2015.03.073>.